Development of a Regenerative Flow Compressor

Prepared by J. Palmer, Engineering Department, 18 December 2020

Scope/Introduction

This report summarizes the development and testing of a prototype regenerative flow compressor (RFC). It includes test data from R&D8121, the original RFC design, as well as data from R&D8177, which were subsequent design iterations based on test results and additional research. A background of the concept of the RFC as well as supporting calculation examples and white paper references are included.

Background

The regenerative flow compressor (RFC) is a rotodynamic machine that transfers energy from a rotating impeller to the fluid in the pump channel via radial blades on the periphery of the impeller. The RFC is also sometimes referred to as a side channel or peripheral compressor. During rotation, the fluid is accelerated in a helical path as it moves through each blade. This allows for multi-staging within a single compressor housing, developing high compression ratios in a single revolution.

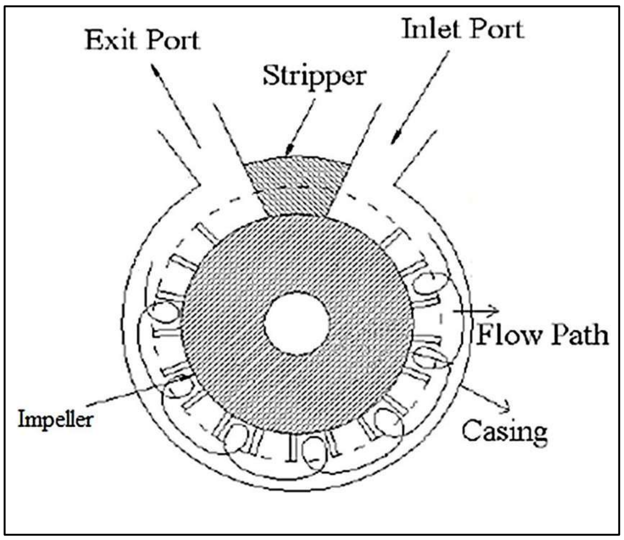

The compressor housing contains a “stripper” that separates the inlet and outlet ports of the compressor. The clearances between the impeller and compressor housing, and more specifically the stripper, are minimized to reduce leakage flow and improve overall system efficiency.

Due to the centrifugal impeller design there are no valves required, as there are no intake or exhaust strokes requiring a “sealed” chamber. This provides a quieter operating compressor with only one moving part, the impeller. This also provides for a simple compressor construction containing fewer components that is more axially compact than a typical diaphragm or piston compressor.

The disadvantages of the RFC are 1) high power consumption and low efficiency under pressure performance compared to a diaphragm or piston pump, and 2) the tight manufacturing clearances required to minimize leakage between the impeller and volute/head faces. However, these required clearances are well within the tolerances of normal CNC machine operations.

The mathematical model for the RFC was developed using Microsoft Excel and a series of complex formulas taken predominantly from the white paper "An Improved Theory for Regenerative Pump Performance" by T. Meakhail and S.O. Park. The Excel calculator requires a series of dimensional inputs describing the compressor shape and the use of the Solver add-in to predict compressor performance one data point at a time, thus allowing theoretical performance curves to be generated. During development, the calculator was modified multiple times as formula/unit conversion errors leading to overly optimistic results were discovered.

The following papers were also heavily referenced during development: "Theory and Design of the Regenerative Flow Compressor" by Abraham Engeda and Mukarrum Raheel; "Review on Modification in Geometry of Regenerative Pump" by Rohit S. Kanase, Ashok T. Pise and Pravin C. Garje; and "A Study of the Peripheral Compressor" by Phillip S. Cates. Additional literature was consulted during development thought not directly used for design evaluation.

Design Theory

The following equations and diagrams detail the calculations required for the development of the RFC. Additional details and explanations can be found in the work of T. Meakhail and S.O. Park.

To create the mathematical model, first the geometry of the impeller and side channel must be determined and the velocity triangles (next figure, ***Determination of the Pump Head***) must be drawn.

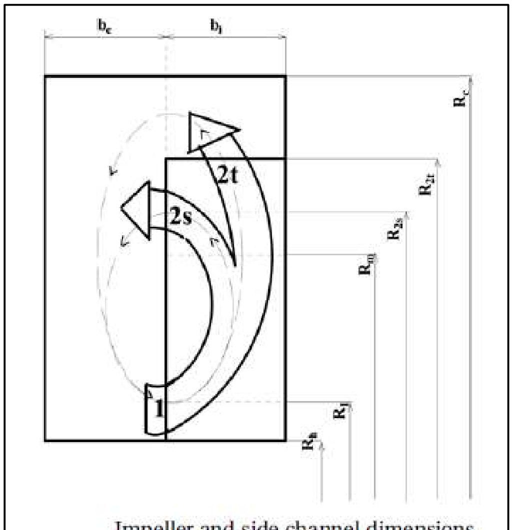

Impeller and side channel dimensions

$$R_m = \sqrt{0.5(R_{2t}^2 + R_{2h}^2)} \qquad R_1 = 0.5(R_m + R_h) \qquad R_{2s} = 0.5(R_{2t} + R_m)$$

where R_h is the hub radius and R_{2t} is the tip radius of the impeller.

Determination of the Pump Head

The head rise of the pump per one circulation, $h_{/cir}$, can be written as

$$gh_{/cir} = \frac{A_{2t}V_{m2t}R_{2t}V_{u2t} + A_{2s}V_{m2s}R_{2s}V_{u2s} + A_1V_{m1}R_1V_{u1}}{R_mA_c}$$

where Vs are the velocities depicted in the above figure and As are the areas defined by

$$A_1 = \pi\left(\frac{R_m^2 - R_h^2}{Z}\right), \quad A_{2s} = \pi\left(\frac{R_{2t}^2 - R_m^2}{Z}\right), \quad A_{2t} = \frac{2\pi R_{2t}b_i}{Z}, \quad A_c = (R_c - R_h)b_c + (R_c - R_{2t})b_i$$

where Z is the number of impeller blades, b_i is the impeller width, b_c is the side channel width and R_c is the outer radius of the side channel.

The term $(A_{2s}V_{m2s}R_{2s}V_{u2s})$ is a function of the side exit angle of the impeller since V_{u2s} is given by

$$V_{u2s} = (U_{2s} - V_{m2s}cot\beta_{2s})$$

and $(A_{2t}V_{m2t}R_{2t}V_{u2t})$ is a function of the tip exit angle of the impeller since V_{u2t} is given by

$$V_{u2t} = (U_{2t} - V_{m2t}cot\beta_{2t})$$

where $U_{2t} = \omega R_{2t},\ U_{2s} = \omega R_{2s}$ and $\omega = 2\pi N/60$.

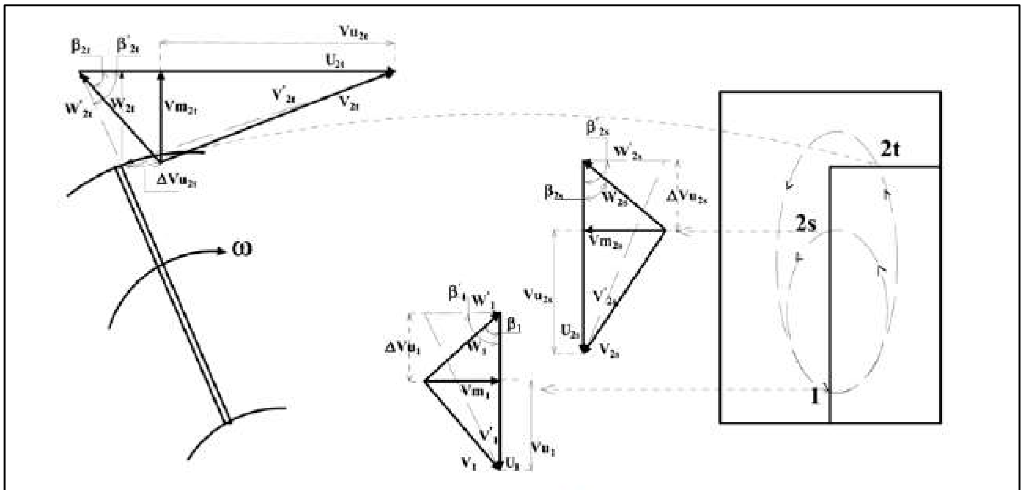

Velocity triangle

To render the velocities more realistic, slip factors need to be considered. For the blade side this factor can be calculated as

$$\sigma_s = \frac{1}{\{1 + 2.5[1 + sin(\beta'_{2s} + 90)]/Z\}}$$

and for the blade tip as

$$\sigma_t = \frac{1}{\{1 + 2.5[1 + sin(\beta'_{2t} + 90)]/Z\}}$$

where β'_{2s} is the blade exit angle at the side and β'_{2t} is the blade exit angle at the tip.

To include the slip factors, the velocity equations can thus be rewritten as

$$V_{u2s} = \sigma_s(U_{2s} - V_{m2s}cot\beta'_{2s}) \text{ and } V_{u2t} = \sigma_t(U_{2t} - V_{m2t}cot\beta'_{2t}).$$

The circulatory flow velocities, V_{m1}, V_{m2s} and V_{m2t} can be calculated using the following equations:

$$\frac{\varepsilon_i}{2sin^2\beta_{2t}}(V_{m2t}^2) + \sigma_t(U_{2t} + U_1)cot\beta_{2t}(V_{m2t}) + \frac{\varepsilon_c}{2}\left(\frac{Q}{A_c}\right)^2 + 2\left(\frac{U_1 Q}{A_c}\right) - \sigma_t(U_{2t} + U_1)U_{2t} = 0$$

$$\frac{\varepsilon_i}{2sin^2\beta_{2s}}(V_{m2s}^2) + \sigma_s(U_{2s})cot\beta_{2s}(V_{m2s}) + \frac{\varepsilon_c}{2}\left(\frac{Q}{A_c}\right)^2 + U_1(2V_c - V_{u2s}) - \sigma_s U_{2s}^2 = 0$$

$$V_{m1} = \frac{A_t V_{m2t} + A_{2s} V_{m2s}}{A_1}$$

The tangential velocity in the side channel V_c can be calculated as

$$V_c = \frac{Q}{A_c}$$

and by assuming that V_c is the average of the tangential components of V_{u1} and V_{u2t}, we have

$$V_{u1} = 2V_c - V_{u2t}$$

The total head of the pump can thus be expressed as

$$H = nh_{/cir} - \frac{1}{2g}K_p\left(\frac{Q}{A_c}\right)^2$$

The head coefficient can be expressed as

$$\psi = \frac{gH}{N^2 D_{2t}^2} - K_p \phi^2$$

where ϕ is the flow coefficient and K_p is the loss coefficient corresponding to the pressure drop in the inlet and outlet ports. K_p is determined experimentally, and as that is not feasible until prototypes are produced and tested, $K_p = 0.01$, previously determined by T. Meakhail and S.O. Park will be used.

The number of circulations n that takes place inside the pump can be calculated from

$$n = \frac{\theta_{eff}}{360} Z$$

where Θ_{eff} is the effective angle of the pump from the inlet port to the outlet port.

Hydraulic Efficiency Losses in the Flow Path

To determine the hydraulic efficiency η_h, power input P_i to the impeller and the real flow rate Q_r must be calculated, taking into consideration the losses inside the pump.

$$\eta_h = \frac{\rho Q_r g H}{P_i}$$

To determine the total power input to the impeller, the friction power loss P_f, the incidence power loss P_{in}, and the power imparted to the impeller P_c must be considered. These values are calculated on a per side basis and must be multiplied by two in the final calculations for a two-sided impeller.

To determine P_f, first the tangential head loss h_c in the side channel must be calculated.

$$gh_c = \frac{1}{2}\varepsilon_c V_c^2$$

where $\mathcal{E}_c$ is the channel skin friction loss given by applying the pipe-loss formula using the concept of hydraulic diameter D_h and the length of the side channel L.

$$\mathcal{E}_c = \lambda_f \frac{D_h}{L}$$

$$\lambda_f = \lambda_o \left[1 + 0.075Re^{0.25}\left(\frac{D_h}{2R_{2t}}\right)^{0.5}\right]$$

$$\lambda_o = 0.316Re^{-0.25}$$

The direct loss in the impeller h_i must be calculated, and it includes losses due to friction, turning, contraction and sudden expansion. It is proportional to the relative velocity in the impeller and is calculated by

$$gh_i = \frac{1}{2}\mathcal{E}_i W_{2t}^2$$

where the loss coefficient $\mathcal{E}_i$ is to be evaluated experimentally. Just as the value of K_p was previously used from the work of T. Meakhail and S.O. Park, $\mathcal{E}_i = 0.65$ will be used for these calculations, as previously determined by the authors.

Before P_f can be calculated, first the meridional (circulatory) flow rate Q_m must be calculated.

$$Q_m = V_{m2t} c_r b_i \theta_{eff}$$

where c_r is the radial clearance between the impeller O.D. and the flow channel O.D.

Summation of h_i and h_c in the impeller provide the total friction power loss as

$$P_f = \rho g Q_m (h_i + h_c)$$

Incidence loss h_{in} is assumed to be caused by the difference between the blade angle and the flow angle when the fluid enters the blade region of the impeller and is estimated as the difference in tangential velocity ΔV_{u1}, which is given by

$$\Delta V_{u1} = (U_1 - V_{u1} - V_{m1} cot\beta_1')$$

where β_1' is the inlet blade angle and $U_1 = \omega R_1$. The incidence loss is then estimated by

$$gh_{in} = \frac{1}{2}\Delta V_{u1}^2$$

The incidence power loss P_{in} can then be calculated as

$$P_{in} = \rho g Q_m h_{in}$$

Input Power to the Impeller

The input power to the impeller is equal to the output power plus the summation of losses within the pump. The total head equation can be rewritten as

$$H = H_c - H_{ic}$$

where H_c is the total head imparted from the impeller to the fluid in the side channel and H_{ic} is the head loss in the inlet and outlet ports.

The power imparted from the impeller P_c can be calculated as

$$P_c = \rho g Q H_c$$

Thus, total input power to the impeller P_i is given by

$$P_i = P_c + P_f + P_{in}$$

Leakage Flow Rate

The real flow rate Q_r required by the pump is less than the flow rate Q through the pump due to the presence of leakage flow Q_l. This leakage flow can be calculated as

$$Q_l = C_d A_{cl}\sqrt{2gH}$$

where C_d is the friction drag coefficient calculated as

$$C_d = \frac{1}{\sqrt{\lambda_f (L/D_h) + 1.5}}$$

and A_{cl} is the total impeller clearance, which for a two-sided impeller is calculated as

$$A_{cl} = t(c_r) + 4R_{2t}c_a$$

where t is the total impeller thickness and c_a is the axial clearance between the impeller faces and pump head/volute faces.

The real flow rate can then be calculated as

$$Q_r = Q - Q_l$$

Equipment Used

The following equipment was used during RFC prototype testing.

Equipment Type	Manufacturer	Model Number	Range	Gauge No.
Rotameter	Rota Yokogawa	RAGN01-G0SS-L633-TTBGN	0.6 – 1.55 L/min	996
Rotameter	Rota Yokogawa	RAGN01-G0SS-L737-TTCGN	1.6 – 3.8 L/min	1087
Rotameter	Rota Yokogawa	-	3.5 – 9.5 L/min	816
Rotameter	Rota Yokogawa			980
Rotameter	Rota Yokogawa		38 – 95 L/min	1089
Stroboscope	Electromatic	PK2X	30 – 12,500 FPM	1091
Multimeter	Fluke	23 III Series	0 – 600 V	145
Multimeter	Fluke	23 II Series	0 – 10 A	146
Pressure Gauge	APG	PG10-100.00-PSIG-N2	0 – 100 PSIG	882
Vacuum Gauge	Cecomp	DPG1000B15PSIA-10	0 – 15 PSIA	827
Sound Meter				807

Compressor Configurations and Estimated Performance

Four different compressor configurations were tested via R&D8121 and R&D8177 to generate the data contained within this report. The dimensional parameters of these configurations are described individually in detail in the tables below and their estimated performance curves are presented.

B3040M-RFC-27x15x9.2

Parameter	Description
R_c	14.50 mm
R_{2t}	13.50 mm
R_h	7.50 mm
t	9.20 mm
b_i	4.00 mm
b_c	4.00 mm
c_a	0.06-0.10 mm
Inlet/Outlet	5 mm HID
Motor Type	Heng Drive B3040M, 12V, 9.4W
Motor P/N	171028
Voltage Tested	9.0-32.0 VDC
R&D No.	R&D8121-1

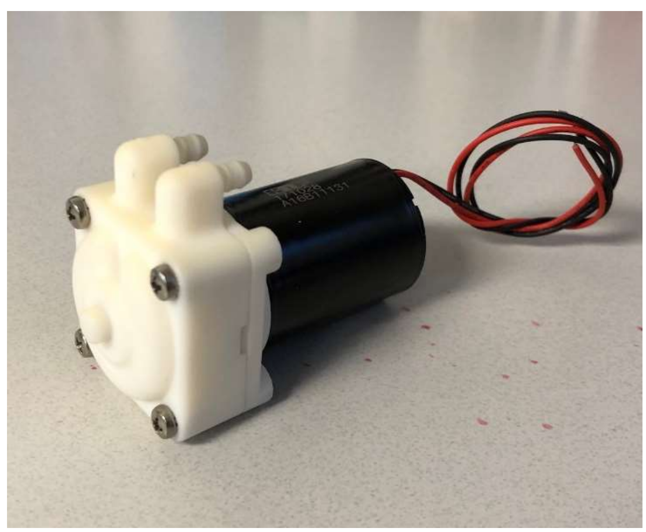

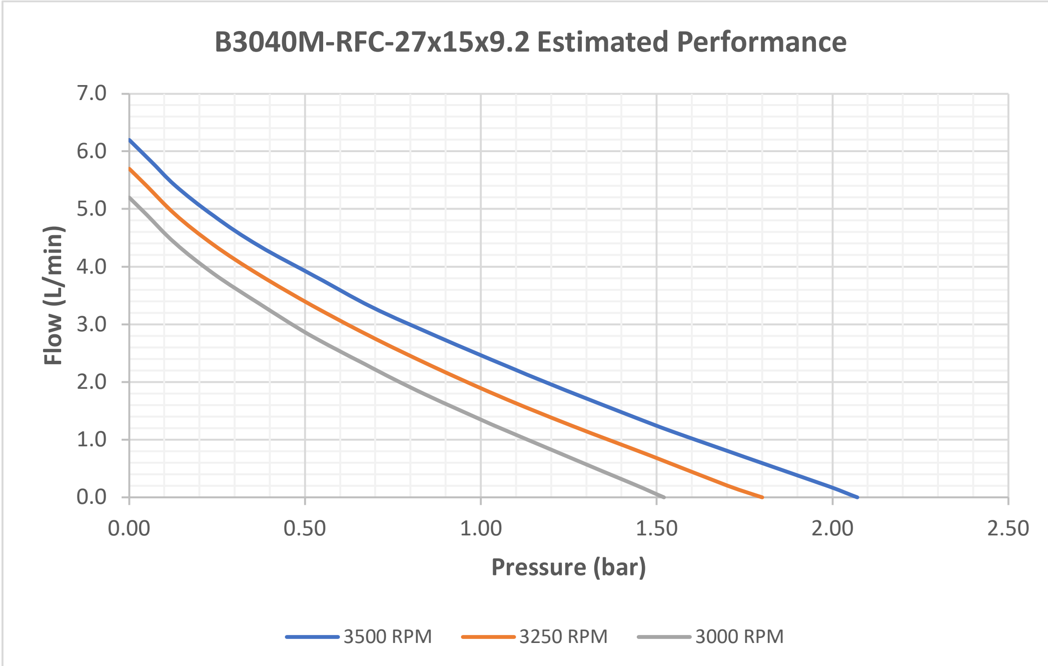

The B3040M-RFC-27x15x9.2 configuration was designed as the Excel calculator was still under development and additional knowledge was still being gathered on the performance characteristics of the RFC. There was a unit conversion error discovered after initial testing that proved this optimistic performance to be unrealistic.

G30-RFC-76x60x11

Parameter	Description
R_c	38.30 mm
R_{2t}	38.00 mm
R_h	30.00 mm
t	10.85 mm
b_i	4.83 mm
b_c	4.00 mm
c_a	0.05-0.15 mm
Inlet/Outlet	3/8 in HID
Motor Type	Dunker G30, 6V, 12.6W
Motor P/N	015336
Voltage Tested	7.0-13.3 VDC
R&D No.	R&D8177-1 to R&D8177-3

While the name of this configuration is G30-RFC-76x60x11, the actual impeller width was machined down to 10.85 mm to allow for axial clearance in the volute, and as such the impeller channel depth was reduced to approximately 4.83 mm. For clarification on the remaining curves, flow vs. pressure is shown as solid lines while power vs. pressure and efficiency vs. pressure are shown as dashed lines.

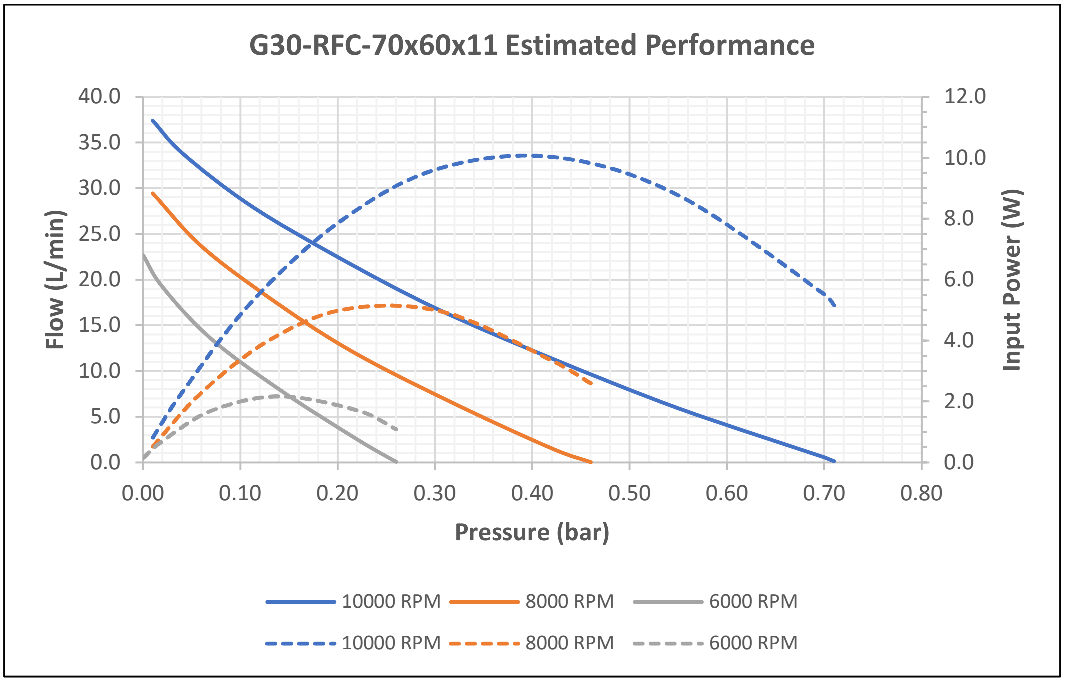

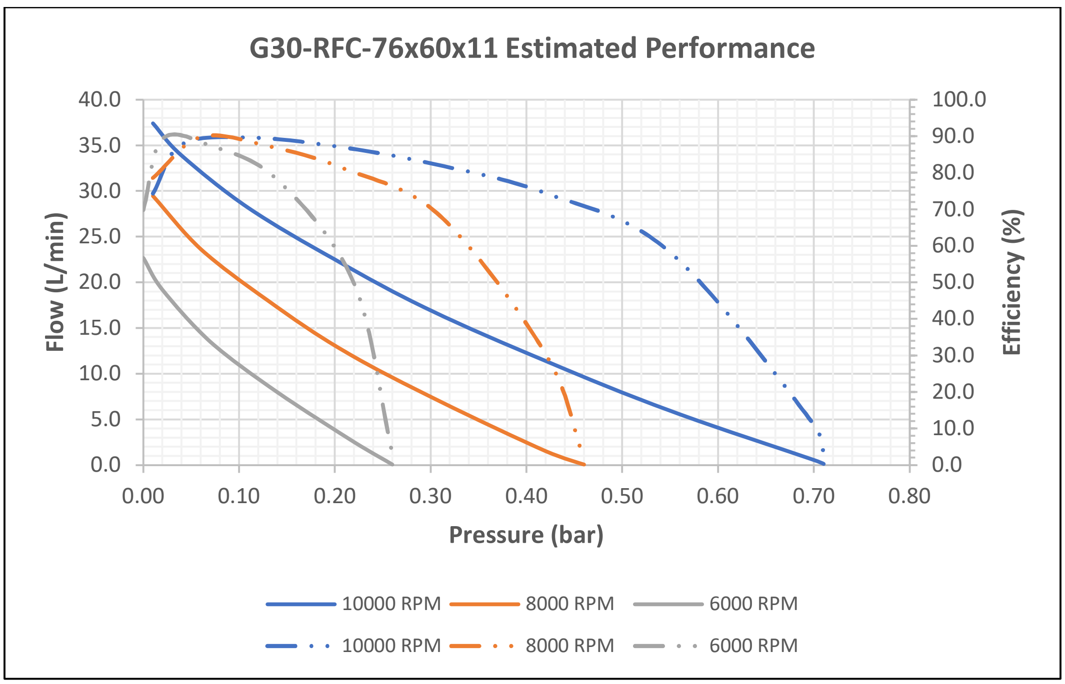

The original G30-RFC-76x60x11 configuration was designed after correcting a unit conversion error in the Excel calculator. This correction showed that higher motor speeds and/or larger diameter impellers would be needed to provide the originally predicted performance. High efficiencies were also predicted based on minimal clearance between the O.D. of the volute and the O.D. of the impeller. As seen in the results section, this didn't quite hold true so a higher power, higher speed motor was sourced from Anaheim Automation.

It is important to point out that the estimated power and efficiency curves presented here are for the compressor end only and exclude the required power input for the motor. The actual power and efficiency curves presented in the ***Results and Discussion*** section are for the complete system since at this time we do not have the ability to measure power and efficiency of only the compressor when de-coupled from the motor.

BLY174S-RFC-76x60x11

Parameter	Description
R_c	38.30 mm
R_{2t}	38.00 mm
R_h	30.00 mm
t	10.85 mm
b_i	4.83 mm
b_c	4.00 mm
c_a	0.15-0.20 mm
Inlet/Outlet	3/8” HID
Motor Type	Anaheim Automation BLY174S, 24V, 113W
Motor P/N	BLY174S-24V-12000
Voltage Tested	24.0 VDC
R&D No.	R&D8177-4

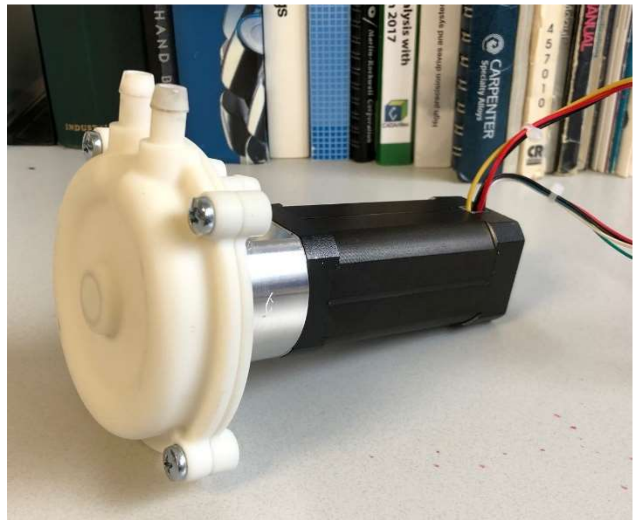

The performance predictions for this configuration were the same as originally estimated for the G30 Dunker motor, except for higher flow and pressure expectations at speeds of 10,000+ RPM. It was theorized that the G30 motor might not have enough power and speed to successfully produce the desired pressure performance since it was being used well outside its nominal range. A set of adapters were produced in the machine shop to allow for the G30-RFC components to be installed on the Anaheim Automation motor, which utilizes a larger shaft and motor flange diameter.

BLY174S-RFC-76x60x11-Gen2

Parameter	Description
R_c	40.50 mm
R_{2t}	38.00 mm
R_h	30.00 mm
t	10.85 mm
b_i	4.83 mm
b_c	3.00 mm
c_a	0.15-0.20 mm
Inlet/Outlet	3/8” HID
Motor Type	Anaheim Automation BLY174S, 24V, 113W
Motor P/N	BLY174S-24V-12000
Voltage Tested	24.0 VDC
R&D No.	R&D8177-5 R&D8177-6

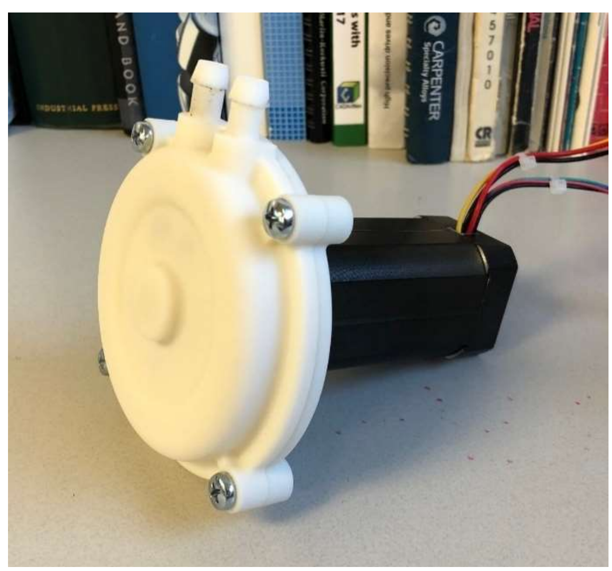

This configuration uses the same impeller as the original G30-RFC design, but machined for a 5 mm shaft diameter to allow for direct mounting to the BLY174S motor. A new volute and compressor head were designed with optimized dimensions to allow the air to more easily flow through the side channel and to better match the dimensions of the previously developed impeller.

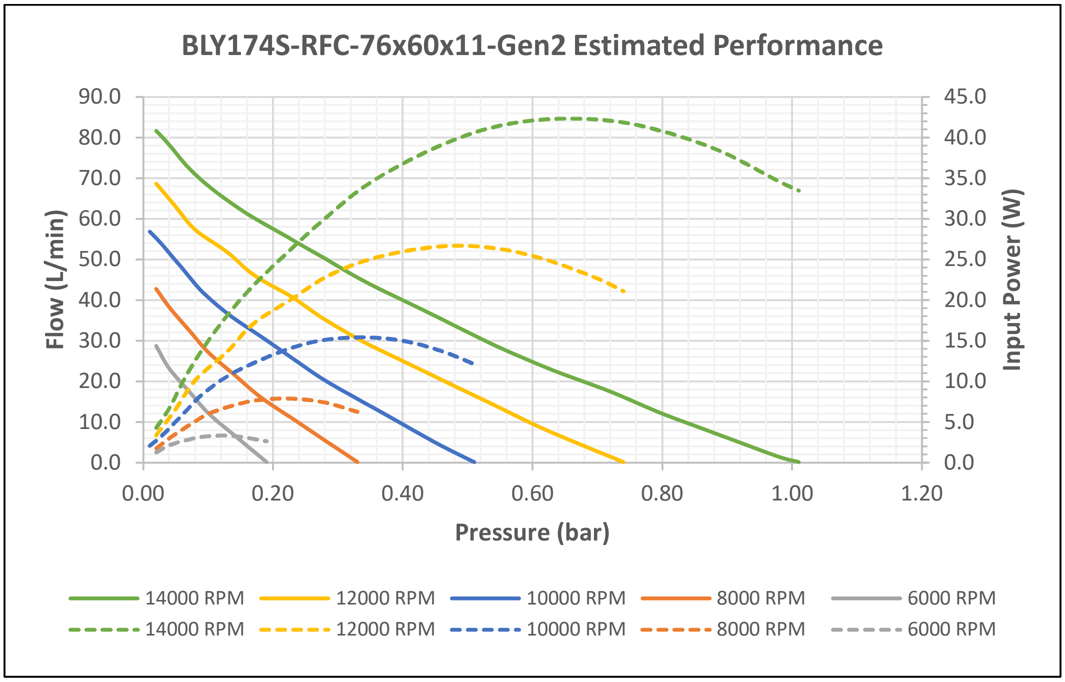

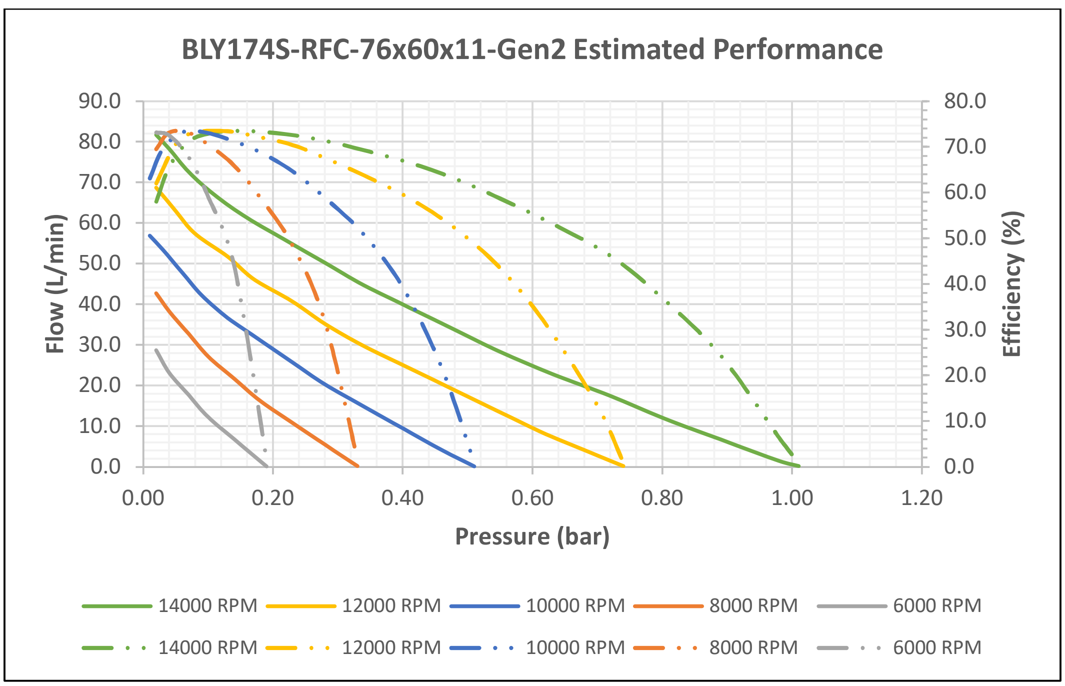

Test Set Up

The compressors were tested using the equipment described in the ***Equipment Used*** section of the report. Different flow meters were required depending on the output of the compressor being tested. The B3040M-RFC and G30-RFC were testing using DC input voltage as the B3040M motor has a built-in BLDC controller and the G30 motor is a standard DC motor. The BLY174S motor is a BLDC without a built-in controller, so the standard 10A controller was used with full control settings to regulate output speed and current draw to avoid damaging the motor.

Results and Discussion

The results of each compressor configuration are presented individually, starting with the B3040M-RFC.

B3040M-RFC-27x15x9.2

The results for this configuration were completely underwhelming and don't warrant an actual performance curve, namely because not enough data was captured to generate one. Results for this configuration were a free flow of 0.95 L/min and maximum pressure of 0.004 bar at 9500 RPM.

After testing, a mistake was discovered in the Excel calculator that used the wrong conversion between meters of head and bar, which is where the overly optimistic low speed predictions stemmed from. It was later determined that this compressor would likely have to spin at approximately 43,000 RPM to produce the flows and pressures originally predicted.

G30-RFC-76x60x11

This configuration proved much more promising with the ability to generate relatively high free flows when run at 6000, 8000 and 10,000 RPM. In fact, the free flows recorded were actually higher than the original predictions, even with the axial clearance c_a as high as 0.15 mm versus the desired 0.05 mm. Unfortunately, the pressure performance was still well below the predictions.

The Dunker G30 motor used here was a 6 VDC motor with a nominal speed of 4300 RPM. For this application, the motor was supplied with 7.0-13.3 VDC to increase the speeds to those mentioned previously. It was thought that one cause of the lack of performance could be due to running this motor well outside its normal operating range, and thus running up against a "power wall". However, this theory was debunked after testing with the BLY174S motor and making another discovery relating to ideal impeller/volute dimensional ratios.

The performance curves shown below are for input power to the complete system, not power consumption of the compressor alone. Since motor efficiency curves for the motor at this speed are not readily available, it's difficult to determine power consumption of the compressor and motor separately. It is also important to point out that the performance curves shown below are completely straight lines versus the curves shown in the performance estimations. This is due to capturing data points at only free flow and maximum pressure, which naturally draw a simple straight line.

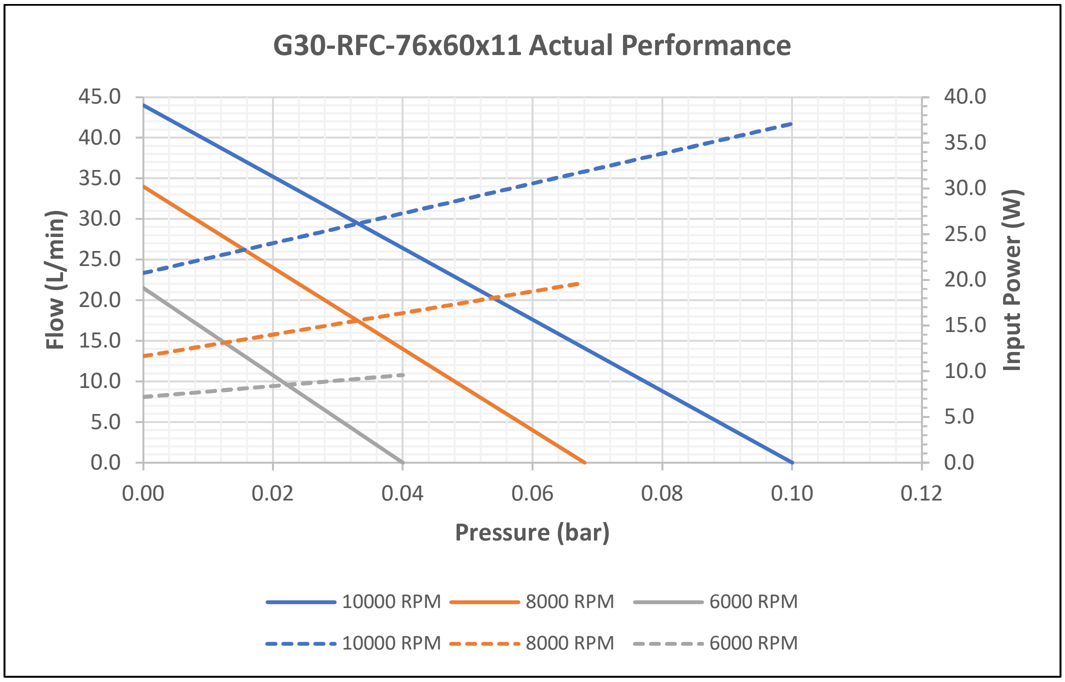

BLY174S-RFC-76x60x11

This configuration allowed for higher speeds to be run more reliably as the BLY174S motor is a 24.0 VDC motor with a nominal speed of 12,000 RPM. Using the standard 10A BLDC controller, speeds of 6000-15,000 RPM were tested, though 15,000 RPM was only tested at free flow as this speed caused rubbing between the impeller and compressor head under load. 15,000 RPM free flow performance (not shown on the chart) was 65.0 L/min. Once again, output pressure was significantly lower than predicted.

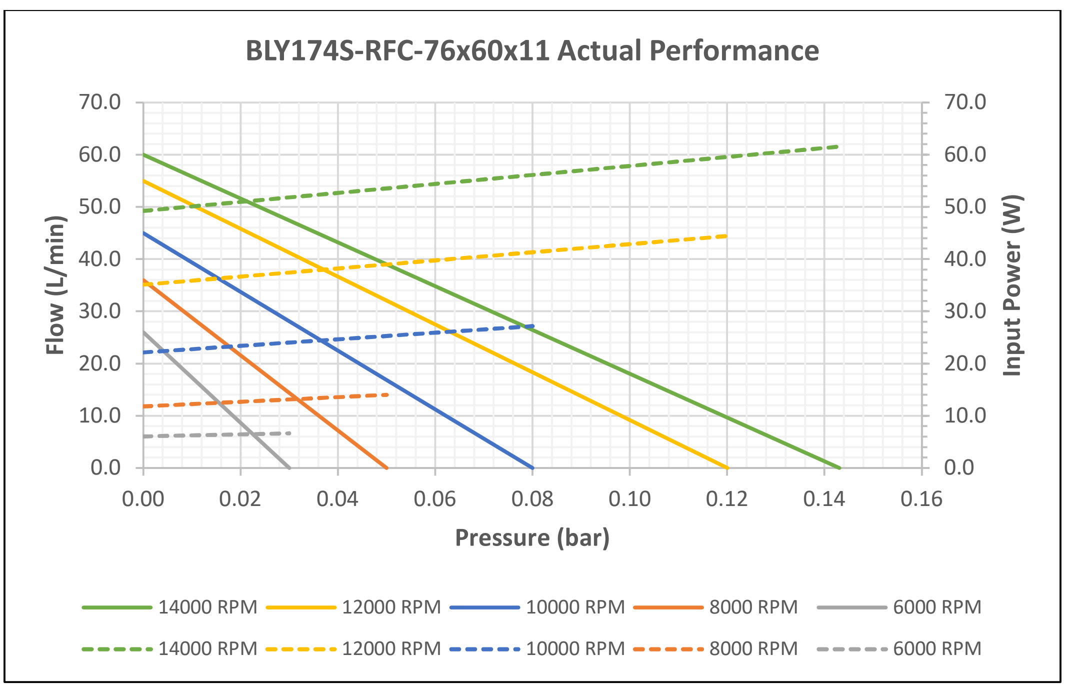

Axial clearances for this iteration were increased to 0.15-0.20 mm to avoid rubbing at higher speeds under load. These larger internal clearances could possibly explain the slightly lower pressure output per RPM seen between the G30-RFC and BLY174S-RFC tests, though it may just be margin of error or assembly variation since the pressure range is so low.

Vacuum performance was also tested with this and as to be expected based on pressure performance, the maximum vacuum was not very impressive. However, the vacuum curves do seem to be mirror images of the pressure curves in terms of absolute values, which indicates the potential for an RFC to generate low vacuum when high pressure is also achieved. It is suspected vacuum performance will ultimately be limited by internal impeller and head/volute clearances.

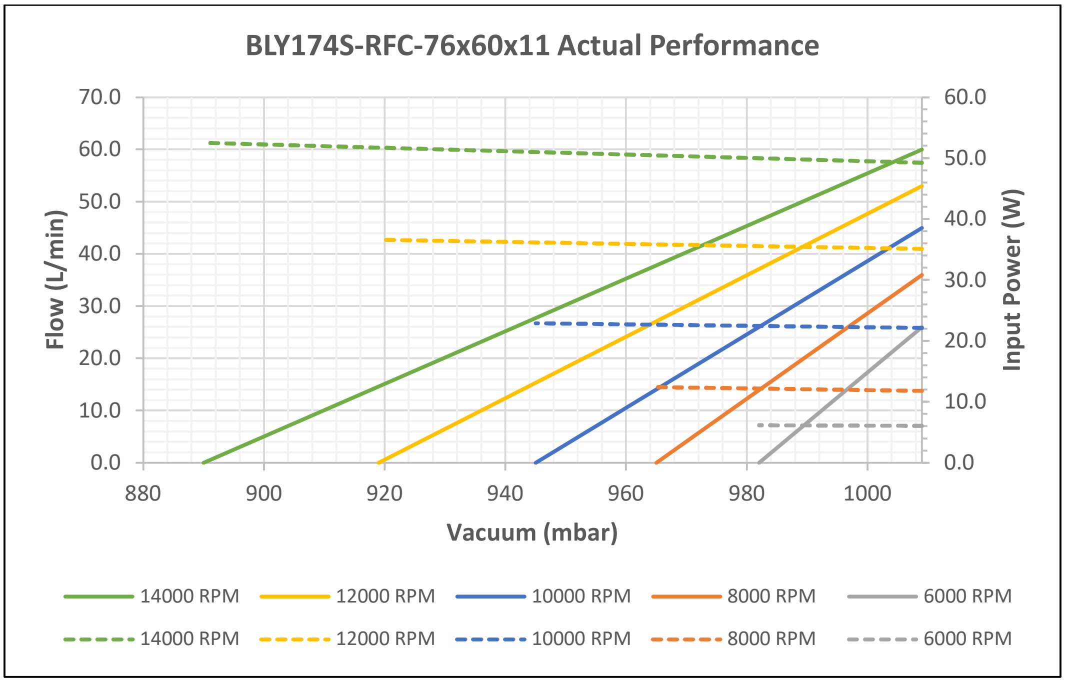

The above BLY174S-RFC curves and those that follow for the Gen2 iteration show input power with approximate motor and controller losses subtracted to clarify the power consumption of just the compressor end. The efficiency curve for the motor, as provided by Anaheim Automation, along with the calculated electrical power losses used can be found in Appendix B.

It is important to point out the presence of additional power consumption that is not accounted for in the Excel calculations but is included in these curves. This additional power required is from the torque of the spinning impeller at various speeds, acting like a flywheel. Because mass and torque are constant, the power draw increases as speed increases. It should be noted that the power draw of the spinning impeller at speeds below 10,000 RPM is greater than the measured input power minus the electrical losses. This is likely due to the mass of the impeller (via the flywheel effect) helping compressor performance at slower speeds. Subtracting the impeller power from the previously calculated input power drives the results negative below 10,000 RPM, so it will be ignored during review of the BLY174S-RFC results. The calculated flywheel power values can be found in Appendix B.

Prior to testing the first BLY174S iteration, a discovery was made relating to proper dimensional ratios between the impeller and the flow channel. It is now understood that as a general rule of thumb the following equations govern an RFC with predictable performance and high efficiency:

$$b_i = \frac{R_{2t} - R_h}{1.5} \qquad b_c = 0.6b_i \qquad R_c = R_{2t} + \frac{1}{2}b_i$$

where the variables are the same as those previously presented in the ***Design Theory*** section.

Taking these formulae into consideration and reviewing the design of the volute and compressor head from the original G30-RFC configuration, it became clear that a mistake was made in the form of a mis-match between the impeller blade profile and the volute/head profile. The impeller was designed with a straight, radial blade profile, which appears to be most common in industry today, while the volute/head were designed with a semi-circular or half-torus profile.

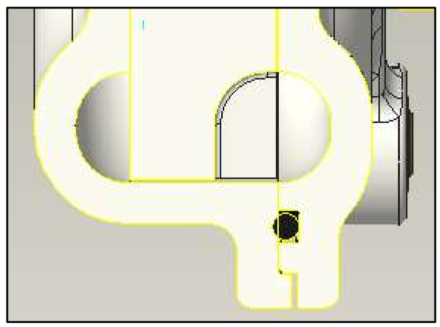

It was theorized that these two profiles cannot be mixed, or the pressure developed in the impeller will dissipate almost immediately as it crashes into the outer wall of the tightly fitted volute. The air does not have the space to follow the helical trajectory created by the RFC unless the impeller and volute/head profiles are matched as shown below.

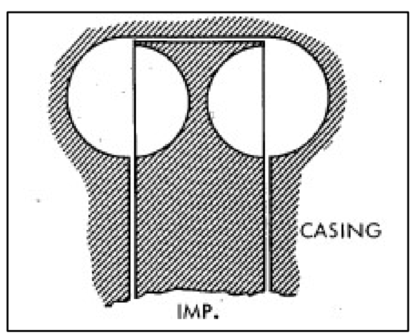

It is worth pointing out that while far less research and testing have been performed on semi-circular blade profiles compared to straight radial blades, it has been proven that total pump output pressure and efficiency are increased with semi-circular blades.

BLY174S-RFC-76x60x11-Gen2

Unfortunately, the results of this configuration were still not quite as predicted. While free flow increased by approximately 20-25% at all speeds (as predicted in the calculations), maximum output pressure decreased by approximately 20-25% at all speeds. The theory that increasing the gap between the O.D. of the impeller (R_{2t}) and the I.D. of the channel (R_c) would allow for additional pressure to be generated was incorrect. However, the new design directly coupled to the motor did allow for additional performance points to be measured at 15,000 RPM without internal rubbing.

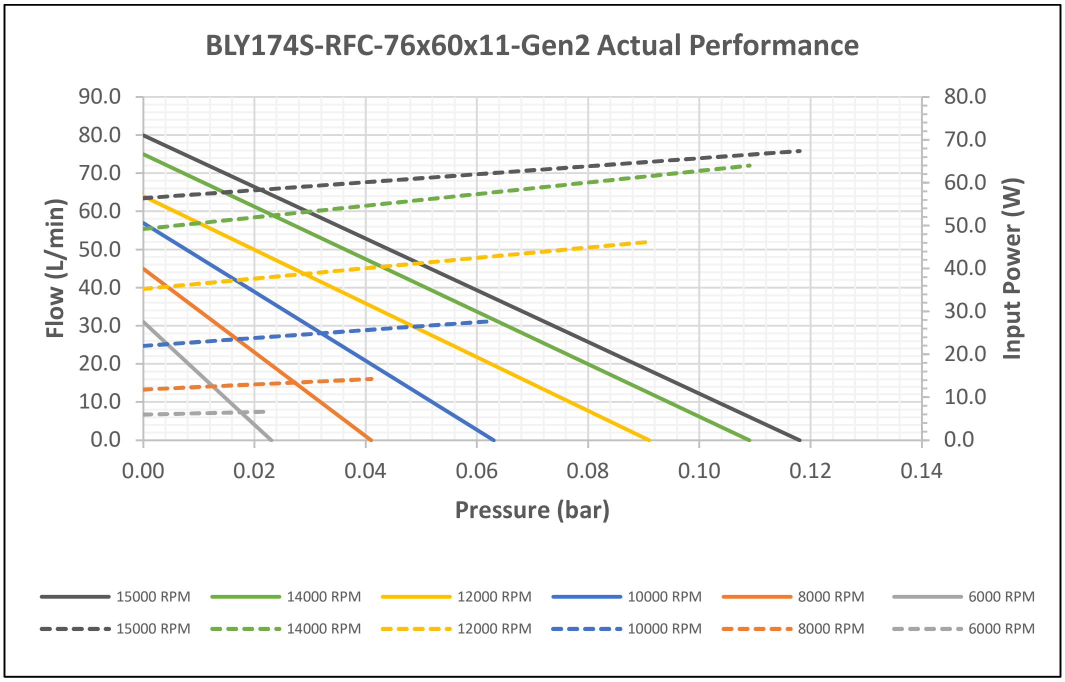

As expected, vacuum performance was also lower and once again was basically a mirror image of the pressure performance.

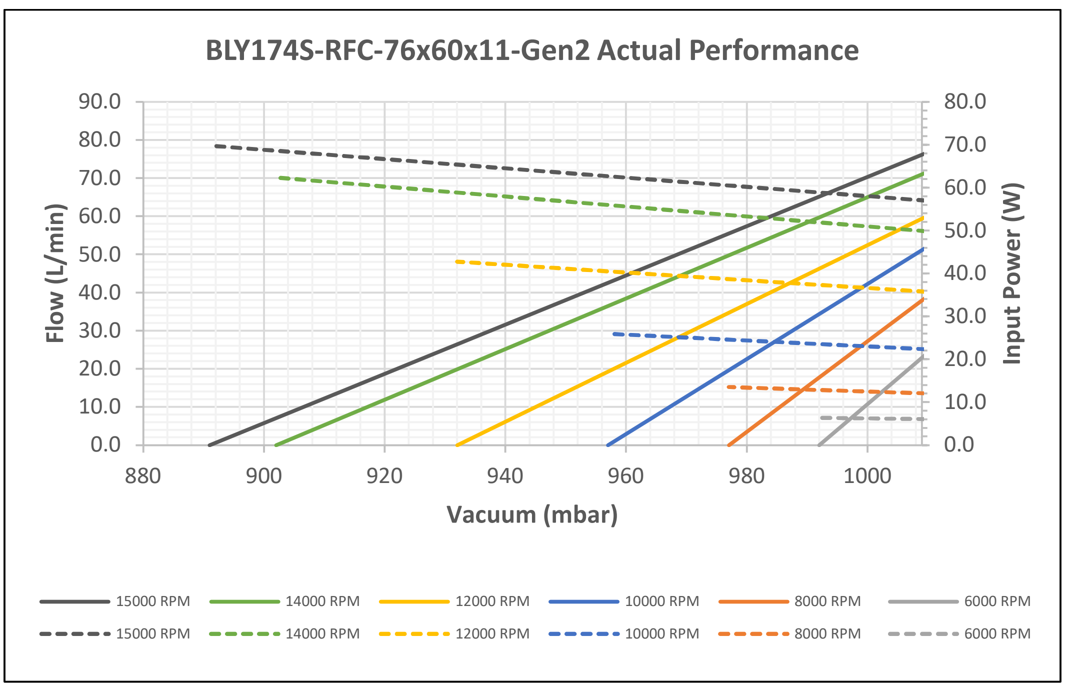

After the realization that the Excel predictions were incredibly optimistic in terms of pressure performance, the calculations were thoroughly scrutinized to root out any errors. After zero errors were found after multiple reviews, focus was placed upon the value of the loss coefficient in the impeller, $\mathcal{E}_i = 0.65$ and the loss coefficient of the inlet/outlet ports, $K_p = 0.01$, which were determined by T. Meakhail and S.O. Park.

As expected, varying $\mathcal{E}_i$ produced a much greater effect on the pressure values than varying K_p. Many values were iteratively tested mathematically until arriving at the values of $\mathcal{E}_i = 28.0$ for impeller losses and $K_p = 1.0$ for inlet/outlet port losses. Using these updated coefficients generated calculated output pressure values that aligned within 5-13% of the physical test results, with the variation dependent on compressor speed. A complete Excel simulation was run, and the results are shown below.

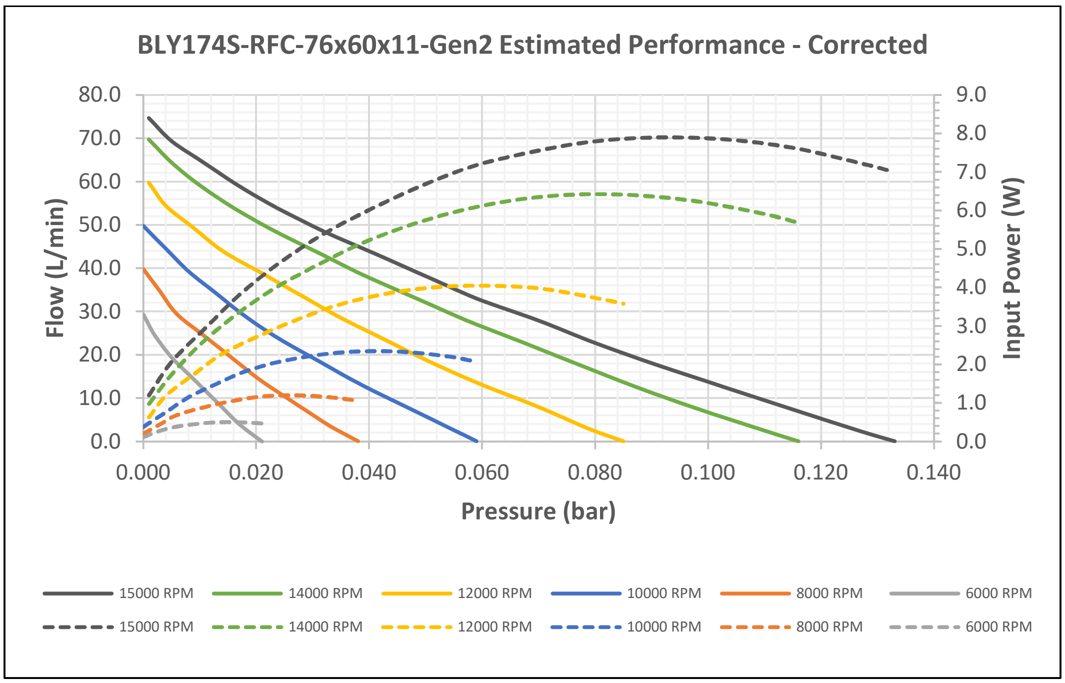

The first thing to point out regarding the curve above is that the mathematical model still produces flow/pressure curves with an actual curvature to them as opposed to the straights lines produced via physical testing. As stated previously in the report, only two points were used to generate the original test curves – free flow and maximum pressure or free flow and maximum vacuum. To confirm if the physical compressor produces curves like shown above, additional points in between the maximums were tested. However, due to limitations of the test equipment and the small delta between free flow and maximum pressure, the additional testing did not yield very useful results.

The second thing to point out is how much lower the calculated input power values are than in the original predictions. These lower power values are directly related to the output pressure of the compressor, as it requires considerably more work to generate pressure than flow with this. Currently confidence is not very high in the calculated power values as they still don't align well with the tested results, even when considering the impeller flywheel losses and the electrical losses of the motor and controller. The deltas between the calculated values and the tested values are shown in the table below, with the range accounting for maximums and minimums.

Speed (RPM)	Calculated (W)	Test (W)	Δ (%)
6000	19.4 / 19.8	14.6 / 16.3	24.7 / 17.7
8000	25.5 / 26.4	23.0 / 27.8	9.8 / 5.3
10000	30.6 / 32.3	34.6 / 43.7	13.1 / 35.3
12000	37.2 / 40.2	50.9 / 66.7	36.8 / 65.9
14000	48.4 / 53.1	72.0 / 93.6	48.8 / 76.3
15000	59.8 / 65.6	90.0 / 107.5	50.5 / 63.9

The calculated values appear to align best at 8000 RPM, but the variation between the other speeds is simply too great to draw any conclusions. This indicates the presence of additional losses not yet accounted for in the calculations. It is possible the source of these losses is due to the heat generated inside the compressor during operation, but that cannot yet be conclusively determined.

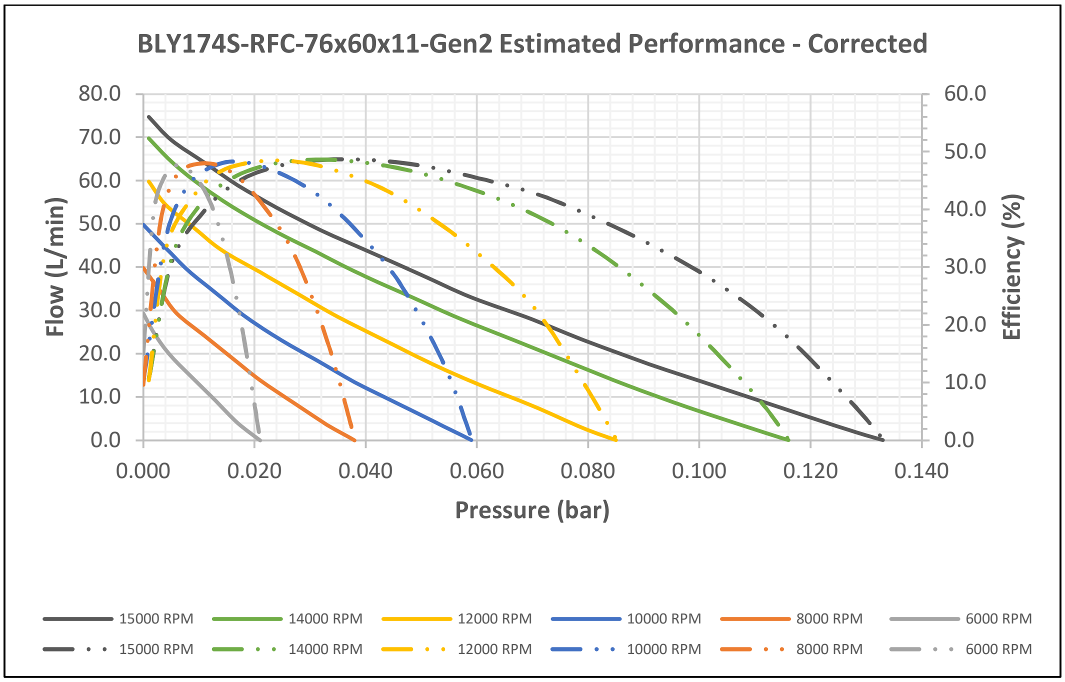

The updated efficiency curve has changed notably with predicted maximum efficiency of 48% versus the original predicted efficiency of 72%. Based on the data available in past and current literature, maximum efficiency for regenerative flow compressors is typically 50% or less, so the updated efficiency curve helps boost confidence in this portion of the mathematical model.

Conclusion and Future Work

This report summarizes the development of approximately one year of work and the results of four different compressor iterations. At the beginning of this project, knowledge was limited regarding the behaviors of regenerative flow compressors other than what was studied in the literature. A common theme in many professional whitepapers (more than the four cited in this report) is that predicting the performance of an RFC is rather difficult without physical testing, even when utilizing computational fluid dynamics. This is consistent with the test results as the mathematical model required modification for better flow/pressure accuracy, but still is likely inaccurate for predicting compressor power.

It was originally thought that an ultra-compact, low-speed compressor could deliver impressive flow and pressure with low power consumption. This has proven to be incorrect from a pressure and power standpoint, but the RFC has proven itself as a worthy and simple solution to high flow at low pressure, while remaining smaller in size compared to a diaphragm pump of similar capacity. Fewer moving parts and no wearing components within the compressor are still advantages over a diaphragm pump.

There are a few steps that should be taken next to further understand the operation of the RFC and to determine its feasibility for additional applications. First, a simple, low-cost experiment is to try using a "reverse-scroll" volute with matching reverse-scroll compressor head to generate additional pressure. The concept of the reverse-scroll is that the cross-sectional area of the flow channel is reduced from inlet to outlet, thus forcing the air to compress more than with a flow channel of constant cross-section. It is not expected that the pressure rise would be much – maybe in the 10-20% range at best – and it is not possible to calculate without using computational fluid dynamics. To test this theory would cost around $200 for a new volute and compressor head if using 3D printed components like the current BLY174S-Gen2 assembly. An example of a reverse-scroll volute is shown below.

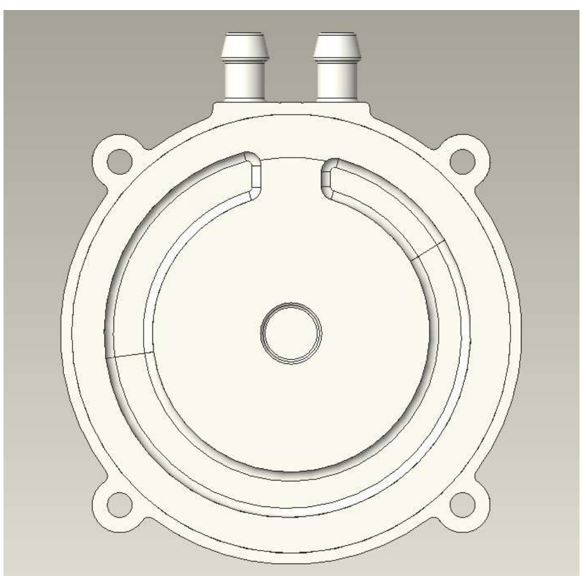

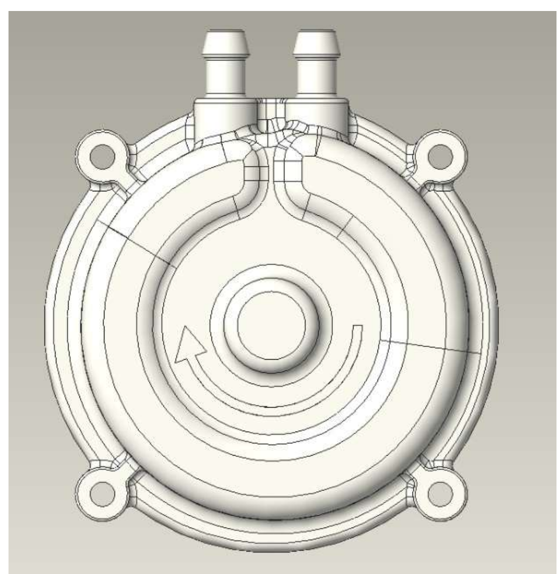

A second low-cost experiment is to develop a pneumatic set that uses semi-circular impeller blade profiles. This design theoretically reduces the tendency of the air to crash into any sharp corners inside the compressor by forcing the air to move in a circular pattern versus an elliptical pattern, and according to the limited literature improves overall efficiency. It is unknown how well the Excel model can predict this performance since the model was developed for use with straight radial blades. A compressor could be developed that utilizes the same diameter impeller as the BLY174S-Gen2 to provide similar flow capacity. To test this theory would cost around $300-400 for a new volute, compressor head and impeller if using 3D printed components.

A third experiment is to build a high speed, machined aluminum prototype compressor to determine how well the current Excel model scales for speed and size based on the new loss coefficients. A simple version with limited machining was developed to test the concept. The proposed design will have the following parameters:

Parameter	Description
R_c	25.00 mm
R_{2t}	23.50 mm
R_h	19.00 mm
t	7.20 mm
b_i	3.00 mm
b_c	1.80 mm
c_a	0.15 mm
Inlet/Outlet	G1/8 w/hose barb
Motor Type	Anaheim Automation BLU09S, 24V, 84W
Motor P/N	BLU09S-24V-34400

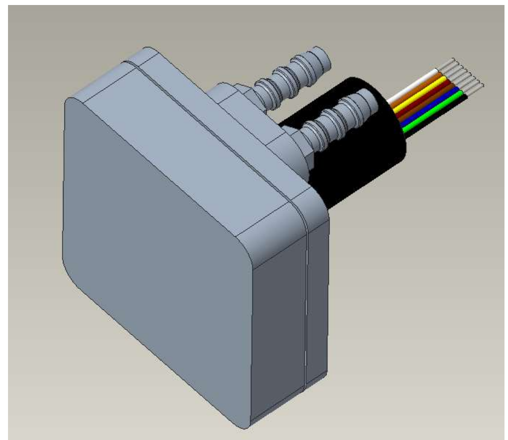

A complete simulation was performed on the proposed design at five different motor speeds and the results are shown below. Output pressure is expected to be more than double that of the BLY174S-RFC-Gen2 design due to significantly higher speeds and maximum efficiency falling at 50% and under agrees well with the updated BLY174S simulation and the literature.

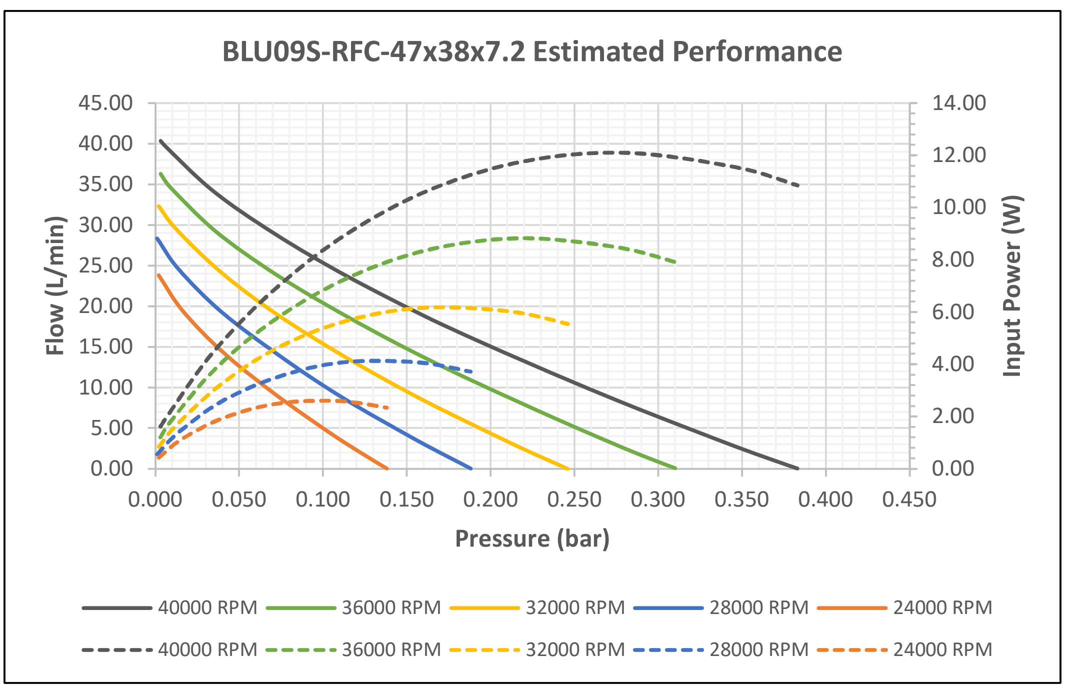

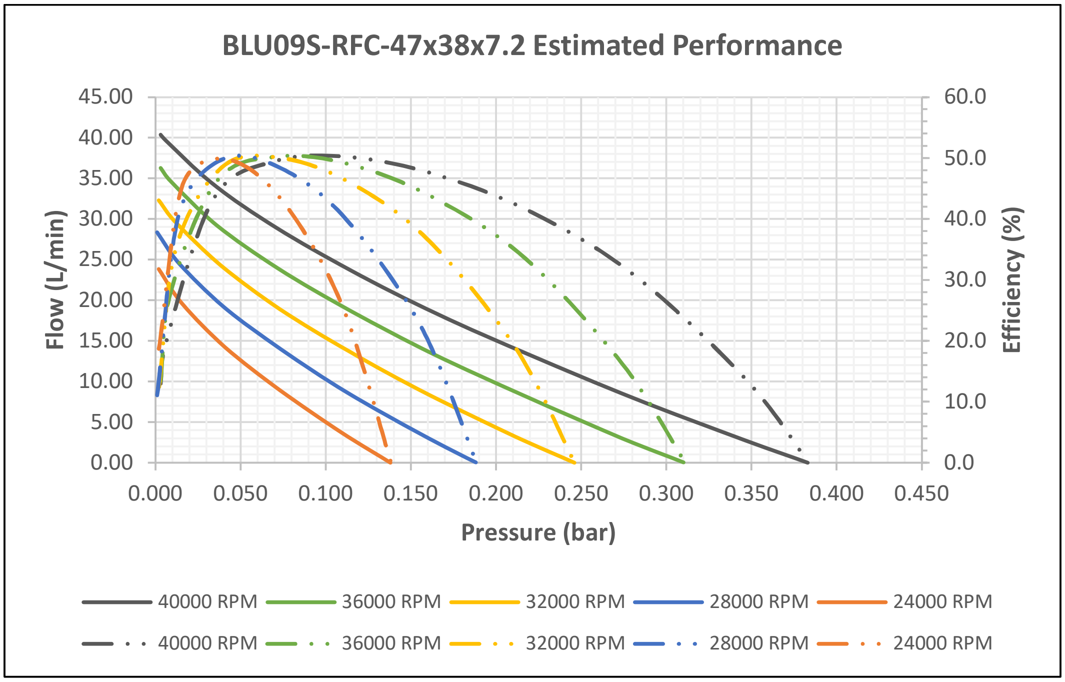

The physical size of this new compressor configuration is quite small at roughly 64 mm x 64 mm x 64 mm, which is a smaller overall package size than an N96 but with flow capacity like an N838, albeit at lower pressure. The motor is very compact with a 22 mm diameter frame size rated at 84 W and is an off the shelf item from Anaheim Automation. Testing this configuration would require new pneumatic set (made overseas for reduced cost), an Anaheim Automation motor, Anaheim high speed controller and digital tachometer at a total approximate cost of $1200.

A final experiment, pending the outcomes of the first three, is to develop a two-stage compressor design to generate greater output pressure. Theoretically using two impellers and flow channels of equal cross-sectional area should double the output pressure of the single-stage design. It is thought possible to generate additional pressure by reducing the flow channel cross-sectional area of the second stage, following a similar principle to that of the reverse-scroll volute concept. This would likely reduce flow capacity and it is unknown what effect this would have on compressor efficiency and power. No cost estimates have been made yet as this design concept has not been reviewed in depth.

References

Meakhail, T. and **S.O. Park** (2004). “An Improved Theory for Regenerative Pump Performance.” *Proc. IMechE Part A: J. Power and Energy*, 2005, Vol. 217, 213-222.

Garje, P.C., Kanase, R.S. and **A.T. Pise**. “Review on Modification in Geometry of Regenerative Pump.” *Journal of Advances in Science and Technology*, 2017, Vol. 13, Issue 1, 362-369.

Engeda, A. and **M. Raheel**. “Theory and Design of the Regenerative Flow Compressor.” *Proceedings of the International Gas Turbine Congress*, 2003.

Cates, P.S. “A Study of the Peripheral Compressor.” *A Thesis Presented to the Graduate Council of the University of Tennessee in Partnership with the Union Carbide Corporation Nuclear Division*, 1966.

Appendix A – Variable Notation and Subscripts

Notation

A	Cross-sectional area
b	Width of the impeller or channel
c	Clearance, radial or axial
D	Diameter
g	Gravitational acceleration
h	Head loss
H	Head
L	Length
n	Number of circulations
N	Rotational speed (RPM)
p	Pressure
P	Power
Q	Flow Rate
R	Radius
U	Peripheral velocity
V	Absolute velocity
W	Relative velocity
Z	Number of impeller blades
β'	Blade angle (theoretical angle of the flow)
β	Flow angle (actual angle of the flow)
ε	Friction loss
η_h	Hydraulic efficiency
ρ	Density
σ	Slip factor
θ_{eff}	Effective pump angle from inlet port to outlet port
ω	Rotational speed (Rad/sec)
Φ	Flow coefficient $(Q/A_c R_m \omega)$
ψ	Head coefficient (gH/N^2D^2)

Subscripts

1	Position of inlet flow to impeller blade
$2s$	Position of outlet flow from impeller side
$2t$	Position of outlet flow from impeller tip
a	Axial
c	Channel
cir	Circulation
h	Impeller hub
i	Impeller
in	Incidence
m	Meridional (circulatory) component, mean value
r	Radial
s	Side
t	Tip
u	Tangential component

Appendix B – System Losses

BLY174S speed/torque curve

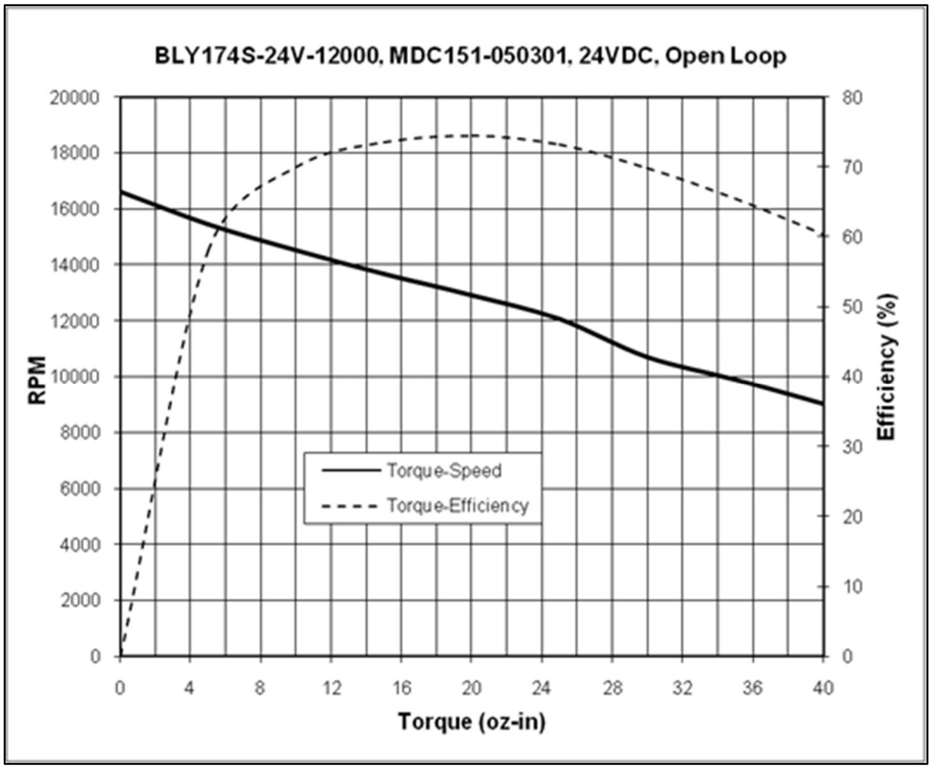

Motor/controller efficiencies and power consumption

Speed (RPM)	Motor Eff. (%)	Controller Eff. (%)	Power (W)
6000	43	95	8.8
8000	54	95	11.2
10000	67	95	12.6
12000	73	95	15.5
14000	72	95	22.8
15000	66	95	32.2

Impeller (flywheel) power consumption

Speed (RPM)	Power (W)
6000	10.5
8000	14.1
10000	17.6
12000	21.1
14000	24.6
15000	26.4